Magnetic Resonance in Medicine 44:602–609 (2000)

Partially Parallel Imaging With Localized Sensitivities (PILS)

Mark A. Griswold,[1*] Peter M. Jakob,[1] Mathias Nittka,[1] James W. Goldfarb,[2] and Axel Haase[1]

In this study a novel partially parallel acquisition method is presented, which can be used to accelerate image acquisition using an RF coil array for spatial encoding. In this technique, Parallel Imaging with Localized Sensitivities (PILS), it is assumed that the individual coils in the array have localized sensitivity patterns, in that their sensitivity is restricted to a finite region of space. Within the PILS model, a detailed, highly accurate RF field map is not needed prior to reconstruction. In PILS, each coil in the array is fully characterized by only two parameters: the center of coil's sensitive region in the FOV and the width of the sensitive region around this center. In this study, it is demonstrated that the incorporation of these coil parameters into a localized Fourier transform allows reconstruction of full FOV images in each of the component coils from data sets acquired with a reduced number of phase encoding steps compared to conventional imaging techniques. After the introduction of the PILS technique, primary focus is given to issues related to the practical implementation of PILS, including coil parameter determination and the SNR and artifact power in the resulting images. Finally, in vivo PILS images are shown which demonstrate the utility of the technique. Magn Reson Med 44:602–609, 2000. © 2000 Wiley-Liss, Inc.

Key words: magnetic resonance imaging; RF coil arrays; surface coils; parallel imaging; fast MR imaging

Since the development of the NMR phased array (1) in the late 1980s, multicoil arrays have been designed to image almost every part of the human anatomy. The primary advantage of arrays to date has been their increased signal-to-noise ratio (SNR).

While traditional MRI with array coils has focused on increasing SNR in the same imaging time, several partially parallel acquisition (PPA) strategies have been proposed (2–14). These techniques use spatial information contained in the component coils of an array to partially replace spatial encoding which would normally be performed using gradients, thereby reducing imaging time. In a PPA acquisition, a fraction of the phase encoding lines are skipped compared to the conventional acquisition. A specialized reconstruction is then applied to the data to reconstruct the missing information, resulting in the unaliased full FOV image in a fraction of the time.

The first PPA technique to demonstrate in vivo results was Simultaneous Acquisition of Spatial Harmonics (SMASH) (2). To date, a factor of two to four time savings has been demonstrated in vivo using SMASH with commercially available six element coil arrays (3,4) and up to 8-fold improvements have been achieved in phantoms using specialized RF hardware (5). However, the primary limiting factor in SMASH is a substantial decrease in image SNR at low acceleration factors (6).

Later in 1997, another PPA technique, Sensitivity Encoding (SENSE) (7), was presented. SENSE has been applied to both cardiac (7,12) and head imaging (13) with promising results.

While SMASH and SENSE have both been successfully applied in many areas of MRI, the primary drawback which limits their widespread clinical application is their requirement of accurate knowledge of the complex sensitivities of component coils in the array at each pixel in the image, or at least in a single line in *k*-space, as in the AUTO-SMASH technique (14). In practice, the actual coil sensitivity information is difficult to determine experimentally, due to contamination by both noise and, more importantly, spin density variations.

In this study we present an alternative to these PPA methods which requires minimal a priori knowledge of the RF coil array to reconstruct an image. In this technique, Parallel Imaging with Localized Sensitivities (PILS), it is assumed that the individual coils in the array have localized sensitivity patterns, in that their sensitivity is restricted to a finite region of space. In this study, it is demonstrated that the incorporation of simple coil parameters into a localized Fourier transform allows reconstruction of full FOV images in each of the component coils from data sets acquired with a reduced number of phase encoding steps. This results in an increase in imaging speed similar to those gains actually achieved by other PPA techniques, while maintaining optimal SNR per unit time.

THEORY

Parallel Imaging With Localized Sensitivities

Before discussing the details of the PILS technique, we first review some basics of the phase encoding process used in traditional imaging methods. In conventional Fourier transform (FT) imaging, *k*-space is sampled at a spacing of Δk_y so that the Nyquist Criterion is satisfied for the width of the object, Y (Fig. 1a). We can define an imaging FOV Y_i which corresponds to the FOV sampled along the phase encoding direction. If, for example, the FOV Y_i is chosen to be a factor of two smaller than Y, image aliasing is typically observed along the phase encoding direction (Fig. 1b).

The statements given above assume that an RF coil with uniform sensitivity is used for reception. Image aliasing can be prevented if a coil with local sensitivity is used,

[1]Department of Physics, University of Würzburg, Würzburg, Germany.
[2]Department of Radiology-MRI, University Hospital Nijmegen, Nijmegen, The Netherlands.
*Correspondence to: Mark A. Griswold, Department of Physics, University of Würzburg, Am Hubland, D-97074 Würzburg, Germany.
E-mail: mark@physik.uni-wuerzburg.de

Received 19 October 1999; revised 11 May 2000; accepted 16 May 2000.

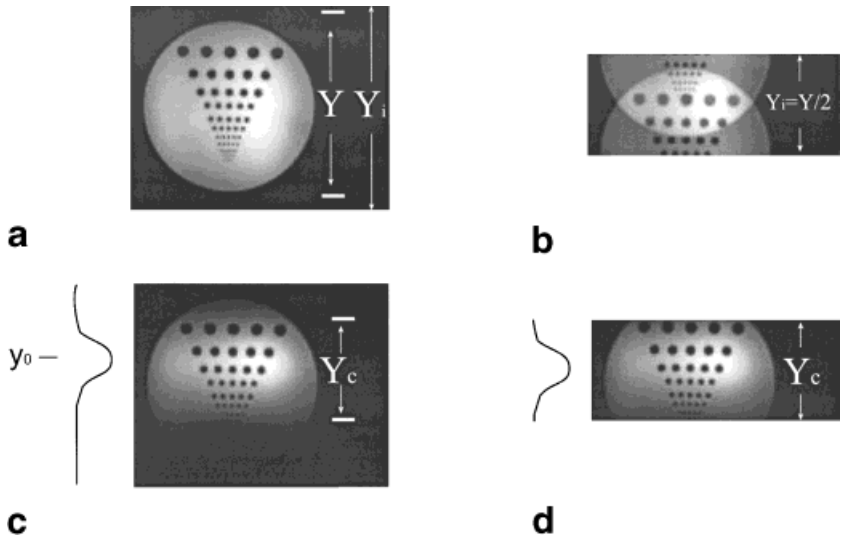

FIG. 1. Single coil imaging. **a:** Definition of the object width Y and the imaging FOV Y_i. **b:** If a FOV of ½ Y is used in the acquisition, image aliasing results. Information is lost in this case due to the overlapping of spatial information. **c:** Imaging with a surface coil restricts the bandwidth of the signal to a range Y_c centered around y_0. **d:** When a surface coil is used for imaging, the FOV in the phase encoding direction can be reduced to Y_c instead of Y without aliasing problems.

such as a surface coil. In this situation, we can treat the RF coil as an analog filter along phase encoding direction that limits the signal to the local imaging FOV Y_c along the phase encoding direction (Fig. 1c). Therefore in the case of this single surface coil, Δk_y can be chosen to sample the FOV Y_c instead of Y (Fig. 1d). Since this image has a smaller FOV, it requires fewer samples compared to the full FOV and can therefore be acquired in a reduced time.

Here we define the *acceleration factor* as the ratio of the sampling spacing in *k*-space needed to sample the full FOV image divided by the sampling spacing used in the small FOV acquisition. This parameter gives the ratio of speed improvement that is obtained using the smaller FOV acquisition instead of the larger FOV acquisition.

The basic idea in PILS is to take this concept of reduced FOV acquisitions in a single coil, and apply it to acquisitions in which smaller FOV images are acquired in parallel in each element of the array. In PILS we view an array of surface coils as a bank of filters, each with an FOV of Y_c, but with a different offset y_o which span Y (Fig. 2a). The primary idea of PILS is to simultaneously collect images in each coil with an FOV of Y_i (less than Y), each corresponding to a different subregion of the full FOV image. We then use the PILS reconstruction process to combine these local image acquisitions into an image with a composite width Y.

To see how the PILS reconstruction process works, we begin with the assumption that each coil has a completely localized sensitivity, such that each coil has sensitivity over Y_c, and is zero everywhere else. The process begins with the acquisition of an image with FOV Y_i simultaneously in each coil of the array, where $Y_c < Y_i < Y$. As can be seen from Fig. 2b, as long as Y_i is chosen to be larger than Y_c, the periodically repeating subimages are completely separated, although the position of the correct subimage is lost. The primary goal of the PILS reconstruction process is to reconstruct only the subimage which is in the correct position in each coil of the array. This process is described in the next section.

The PILS Reconstruction Algorithm

We begin with the simple 1D Fourier transform representation of the MR signal:

$$S(k_y) = \int_{-\infty}^{\infty} \rho(y) e^{ik_y y} dy \qquad [1]$$

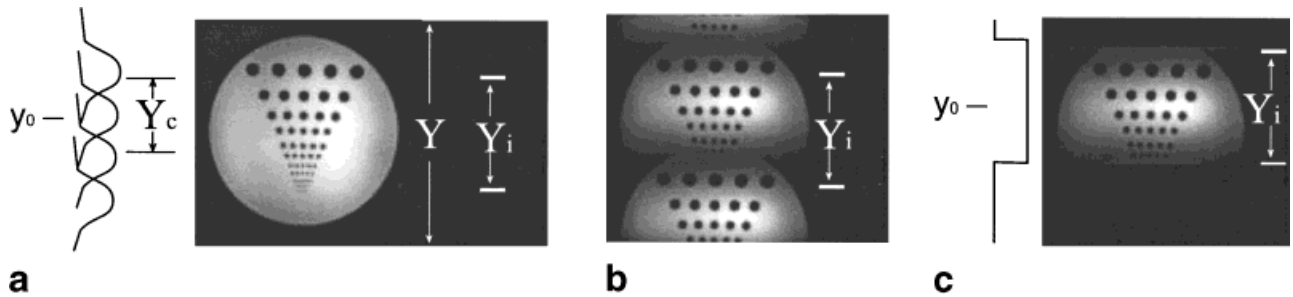

FIG. 2. Imaging with an array. **a:** Definition of Y_c, y_0 and Y_i for an array which spans a length Y. **b:** If an image is acquired with a FOV of Y_i, which is bigger than Y_c, but less than Y, several repeating subimages appear in the full FOV reconstruction, however no overlapping of spatial information occurs, due to the inherent filtering of the surface coil. **c:** In PILS, information about the center position of the signal is incorporated into the reconstruction, and all signal from outside the correct region is suppressed. This results in the correct full FOV image in each component coil.

where ρ(y) is the spin density of the sample along the phase encoding direction and $S(k_y)$ is the received signal. However, if we assume that a coil with localized sensitivity limits the signal to an FOV of Y_c centered around y_o, this integration reduces to:

$$S(k_y) = \int_{y_0 - Y_c/2}^{y_0 + Y_c/2} \rho(y) e^{ik_y y} dy \qquad [2]$$

In the PILS reconstruction, it is assumed that we already have knowledge of the correct location of the center of the coil's sensitive region y_o and the acceleration factor used in the data acquisition. Using this prior knowledge of the range of y values that actually contributed signal in Eq. [2], we can restrict the reconstruction to only have signal in the predefined range of y where the signal originated, such that over the range $y_o - Y_i/2 < y' < y_o + Y_i/2$,

$$\rho(y') = \sum_{K_y} S(k_y) e^{-ik_y y'} = FFT\{\phi(k_y) S(k_y)\} \qquad [3]$$

and is zero everywhere else (Fig. 2c). The term $\phi(k_y)$ is a simple linear phase term needed to correctly shift the center of the reconstructed data to the center of the reconstruction window and is given by:

$$\phi(k_y) = e^{ik_y y_0} \qquad [4]$$

Repeating this process for each coil results in unaliased full FOV images for each coil with signal only in the predefined regions. A composite image can then be reconstructed using any conventional method, such as a sum of squares reconstruction (1).

Many issues need to be considered before this technique can be implemented in practice. Foremost among these issues is the validity of our assumption that the surface coils in the array provide localized sensitivities and that their spatial location can be determined accurately. These practical issues are the focus of the remainder of the manuscript.

METHODS

Computer Simulations

The first question one should ask before implementing PILS is to what extent a surface coil has a localized sensitivity. Typical RF coils have some sensitivity at a large distance from the coil. Therefore, if we assume that sensitive region of a coil is completely limited to a finite region, we guarantee some level of error in the images. The key questions are how large the error is and whether this level of error, or artifact, can be tolerated in a given application.

For this purpose, we have used computer simulations to estimate the artifact power at different imaging FOVs (acceleration factors) for ideal surface coils. To this end, a B_1 field calculation was implemented in the Matlab programming environment (The MathWorks, Natick, MA, USA) using an analytic integration of the Biot-Savart equation. The first simulated coil is a single 5×15 cm loop surface coil. The second simulated array element is a quadrature loop-butterfly pair of the same size. Adjacent coils in both arrays are arranged in the head-foot direction, parallel to the B_0 field of the magnet. For these initial simulations, an image plane parallel to the plane of the coils approximately 10 cm from the coils was assumed. This is approximately the depth that would be optimal in terms of SNR for both of these coils (15).

While these simulated coil profiles give an indication of the localization of the coil sensitivity on a point by point basis, they do not give a global idea of image artifacts introduced by the PILS technique. For this, we return to the analogy of the surface coil as a filter with a pass-band, stop-band, and a transition region in between. We are particularly interested in the amount of power that will contribute to artifacts in the reconstructed image which is a function of the power in the stop-band region of the coil. Given this model, the stop-band rejection was calculated as the power from outside the FOV Y_i versus the power from inside the FOV Y_i:

$$R(Y_i) = \frac{\int_{-\infty}^{-Y_i/2} |C(y)|^2 \, dy + \int_{Y_i/2}^{\infty} |C(y)|^2 \, dy}{\int_{-Y_i/2}^{Y_i/2} |C(y)|^2 \, dy} \qquad [5]$$

where $C(y)$ is the sensitivity of the coil along y with the center of the coil sensitivity centered at y_o=0. This measure can then be used to define a safe imaging FOV (Y_i) that can be used with the array once some level of error tolerance is defined.

Simulated PILS Imaging

Once simulated coil field maps were generated, simulated PILS imaging was performed using an image of a resolution phantom. Simulated images were generated using the four element quadrature array used in the last section. Images were reconstructed at various acceleration factors from one to four and the resulting images were evaluated qualitatively for general image quality with primary attention to residual aliasing artifacts.

The images acquired at integer acceleration factors were then subjected to quantitative evaluation of both SNR and artifact power. SNR was evaluated on a pixel by pixel basis using multiple reconstructed copies of the same image with different received noise in each image, as described in Reference (6). For this study, a series of 30 images was used in this calculation. SNR was then derived as the mean value over the series of images divided by the standard deviation across the series.

Artifact power was evaluated using a noise free reference and a noise free PILS reconstruction. The total artifact power in this case is the total power in the difference image, found by subtracting the reference and PILS images and squaring the magnitude of the result, divided by the total power in the reference image, found by squaring the magnitude of the reference image.

Determination of Coil Parameters and In Vivo PILS Imaging

As stated above, the two coil-based parameters that need to be known prior to image acquisition and reconstruction in

PILS are the center of the each coil's sensitive region, y_0, and the width of the sensitive region around the center, Y_c. The method we have chosen to implement for determination of these parameters in PILS is a relatively simple yet robust one. In this method, the magnitude of a one-dimensional B_1 field profile is acquired in each of the coils and fit to gaussian functions. These profiles can be acquired from either (i) a projection along the phase encoding direction or (ii) a single image line in a full FOV reference image. The position of the maximum of resulting gaussian fit can then be used as the center of the coil sensitivity, y_0, and the full-width half-maximum (FWHM) of the function can be used as the width of each coil, Y_c.

This coil fitting procedure was implemented in actual in vivo experiments and was used to determine the coil parameters for a four-element cardiac array which had previously been designed for SMASH cardiac imaging (16). The array contains four elements, each 7×23 cm, arranged in the head-foot direction. For these in vivo images, a single line from a full FOV reference scan was fit to the gaussian functions.

For initial demonstration of the PILS technique, we applied PILS to routine cardiac imaging[3] on a 1.5T Siemens Vision scanner (Siemens Medical, Erlangen, Germany). A segmented FLASH sequence was used with the four element cardiac array listed above using an incremented flip angle series with nine lines per segment, TR=14.4, TE=7.3, matrix=144×256, FOV=300×300 mm, slice=8mm, number of excitations (NEX) =1. The conventional and PILS acquisitions were performed in separate breathholds. In this case, the conventional fully gradient encoded technique required 16 cardiac cycles to acquire the full image, while the PILS technique required only eight cardiac cycles, corresponding to an acceleration factor of two. After reconstruction of component coil images using the PILS reconstruction algorithm, the component coil images were combined using the sum of squares algorithm.

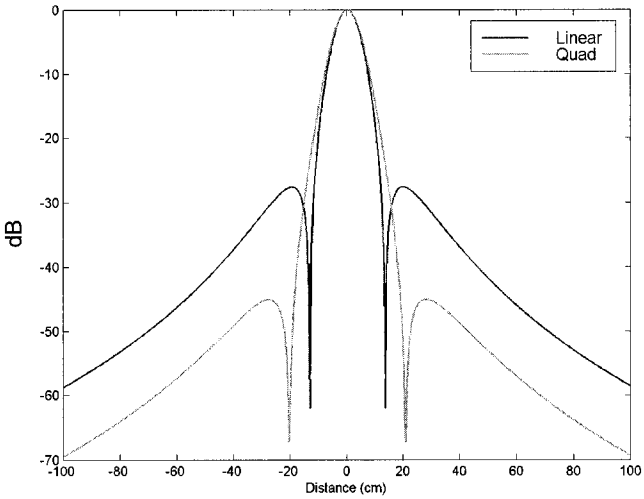

FIG. 3. The profiles along the z-direction are shown for both a linear (black line) and quadrature (gray) coil. Note that both coils achieve a suppression of the out of band signals of over 25 dBs.

RESULTS

Computer Simulations

The resulting sensitivity profiles from the simulated coils are shown in a semi-log plot in Fig. 3. At first appearance the coils have similar profiles in that their B_1 fields are primarily confined to a specific region. However, the region that has the greatest affect on PILS is the region outside of the main lobe of the coils. One side-lobe can clearly be seen in the stop-band region of each coil. However, the height of these sidelobes is at least 25 dB from the height of the main lobe for the loop coil and at least 45 dB down for the quadrature coil. Given these results, it is clear that the assumption of localized sensitivity is valid for these coils.

However, some measure of the global error included in this assumption is needed to determine what the minimum Y_c is for a particular coil. For this we turn to the calculations of stop-band rejection, shown in Fig. 4. This figure shows the stop-band rejection in dBs at various imaging FOVs. The vertical lines on the figure correspond to the FWHM of the coil (left, thin lines) and two times the FWHM (right, thick lines). As can be seen, if the FOV corresponding to the FWHM of the coil is chosen as the imaging FOV, the total out of band power is on the order of 20 dBs less than the in-band power for both coils. However, if an FOV of twice the FWHM of the coils is chosen, the out of band power is significantly reduced. At this FOV, the linear coil has a stop-band rejection of approximately 42 dBs while the quadrature coil shows further suppression at approximately 50 dBs. With these calculations in hand, one can determine a safe imaging FOV (Y_i)

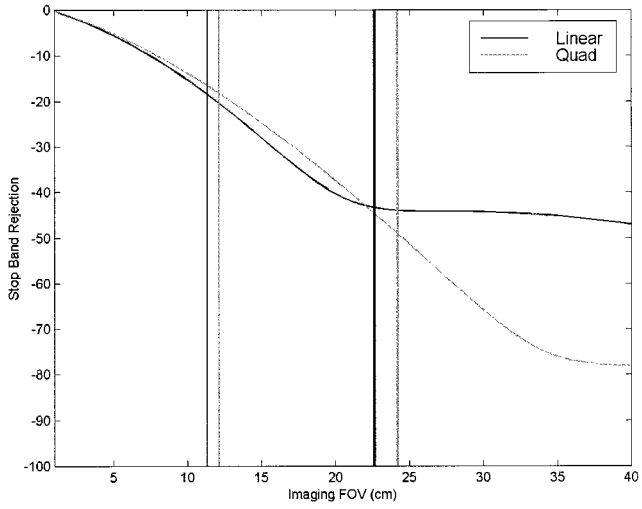

FIG. 4. Shown are the results of the calculation of stop-band rejection vs phase encoding FOV from this study. The thin vertical lines on the left correspond to a FOV equal to the FWHM of the coils. The thicker vertical lines on the right correspond to a FOV of twice the FWHM.

[3]It should be noted that the scans used in this initial data set were first used in a study of cardiac imaging with AUTO-SMASH (14). The corresponding AUTO-SMASH reconstruction of this data set can be found in that reference.

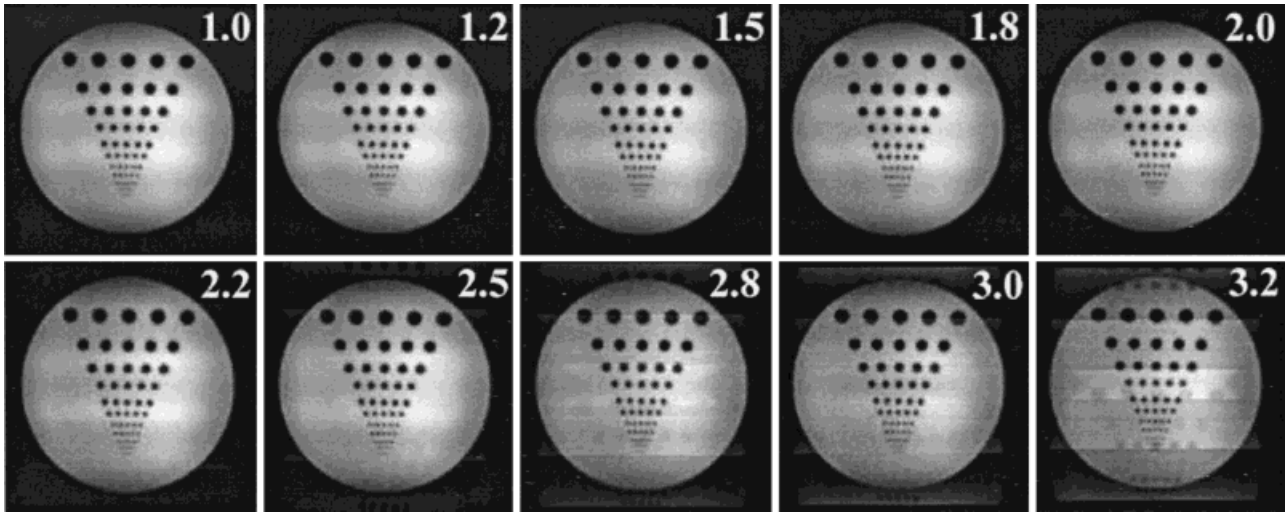

FIG. 5. Simulated PILS images from a four element quadrature array are shown up to a factor of 3.2. Note the excellent image quality achieved up to a factor of 2.2.

that can be used with PILS once some level of expected artifact power is specified for a given imaging application.

Simulated PILS Imaging

The simulated images reconstructed using the PILS technique up to an acceleration factor of 3.2 for the four element quadrature array are summarized in Fig. 5. As can be seen from these images, little or no aliasing is discernable up to an acceleration factor of 2.2. Localized aliasing artifacts are observed when the acceleration factor reaches 3.2. Above this acceleration factor, residual aliasing dominates the image, and image quality is significantly reduced.

For a closer look at the reconstructed images, individual component coil reconstructions are shown for an acceleration factor of 2.5 in Fig. 6. The component coil images obtained from the PILS reconstruction in Fig. 6a highlight a basic mechanism of artifact reduction in PILS. In these simulated reconstructions, residual aliasing is primarily restricted to areas near the edge of each subimage, which are areas that typically have very low signal levels to begin with. These areas on the edge of each component image are typically the areas near the centers of the neighboring coils, which are usually free of artifact. In the composite PILS image, the strong signal coming from the center of one coil's sensitive region tends to diminish the impact of low intensity artifacts in the other component coil images. An example of this effect is highlighted by the white arrows in the component coil images of Fig. 6a. The artifacts in the component coil images are barely detectable in the composite image, due to the strong signal at this location from the adjacent coils. For reference, the conventional sum of squares reconstruction with full phase encoding is shown in Fig. 6b.

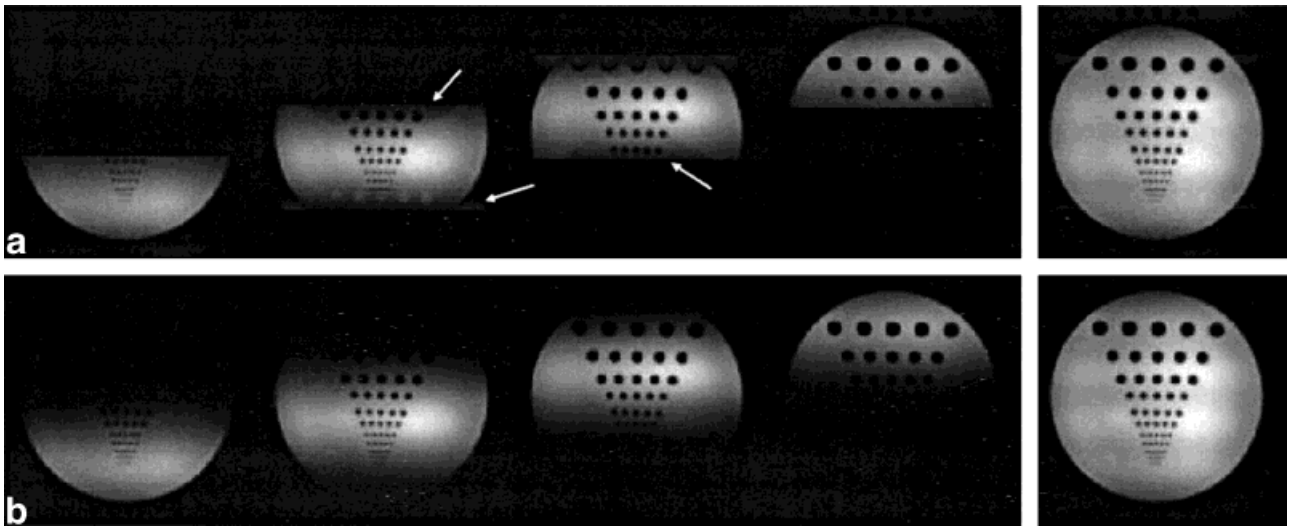

FIG. 6. **a:** Component coil images resulting from the PILS reconstruction acquired at an acceleration factor of 2.5. Note the nearly complete suppression of aliasing artifacts in the composite image (right), even though several of the component coil images show subtle aliasing artifacts (white arrows). **b:** Conventional fully phase encoded reference images.

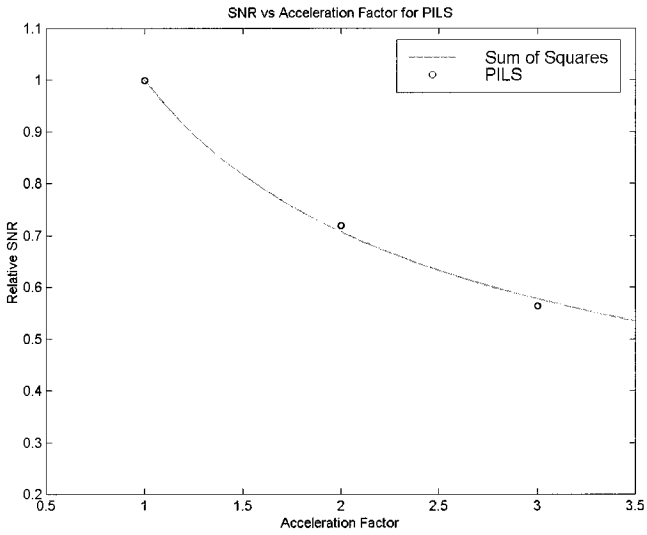

FIG. 7. Signal to noise ratio in PILS vs acceleration factor. The circles represent measured points for PILS. The gray line begins at the SNR measured at an acceleration factor of 1.0. The rest of the line contains the points that would be measured from a conventional sum of squares reference image with the appropriate increase in imaging speed. Note that PILS achieves the same SNR as the reference at all acceleration factors tested.

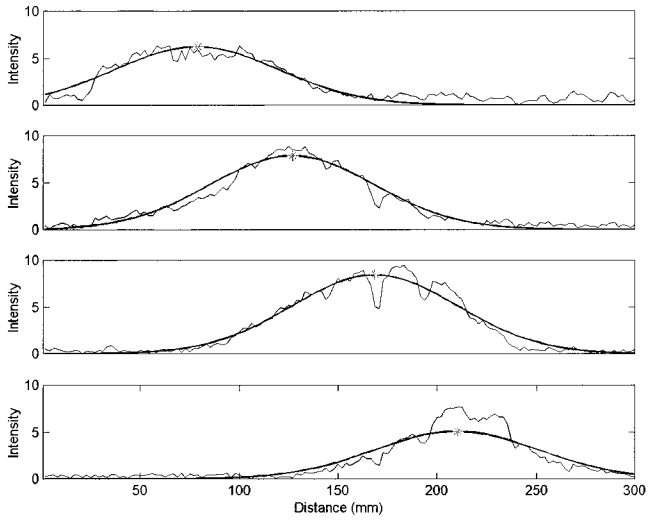

FIG. 8. In vivo coil sensitivity maps used for the images in Fig. 9 (thin lines). The gaussian fit used to determine the coil centers are shown as the thick lines. The points used as the coil centers are shown as gray stars.

The SNR results from the simulated phantom in Fig. 7 and Table 1 demonstrate that up to a factor of three using the four-element array, PILS achieves optimal SNR per unit time compared to the conventional full time acquisitions. This should be expected, since the composite image in PILS is made up of shifted versions of smaller FOV images which have been reconstructed with a conventional FFT.

The artifact power measurements given in Table 1 follow the pattern that is typically found in all PPA techniques. At acceleration factors approaching the number of elements in the array, the images demonstrate increasing artifact power. For the PILS technique, artifact power remains on the order of 1% or less up to an acceleration factor of three. At lower powers, the artifacts would be at a level that in many cases would only be observable in images with high signal to noise ratios, with the total artifact power remaining at a level under 1%.

Determination of Coil Parameters and In Vivo PILS Imaging

The signal profiles in each of the four coils of the array are shown in Fig. 8 as the thin lines in each subfigure. In addition, the gaussian fits used to find the center of each coil are shown as thick lines. The resulting center derived from these gaussian fits are marked with a star.

The component coil images acquired with an acceleration factor of two are shown in Fig. 9a for the PILS reconstruction, while the corresponding fully gradient encoding counterparts are shown in Fig. 9b. As can be seen from this figure, the component coil images that are reconstructed from each coil using the PILS technique closely resemble those that were acquired in twice the time using the conventional imaging technique.

DISCUSSION

In this study, we have presented a novel PPA imaging technique which is easy to implement in practice, easy to understand, requires minimal a priori information about the coil array, and provides optimal SNR at all acceleration factors. In the PILS technique, we view an array of surface coils as a bank of filters along the phase encoding direction. Using the knowledge of the positions of each of these bands in the image, we reconstruct shifted small FOV images which are acquired simultaneously in each array element. These small FOV images are then positioned at the correct locations within an image the size of the full FOV and finally combined into a composite image through normal array reconstruction algorithms. In this study, we have shown that PILS can provide acceleration factors up to 2.2 with few noticeable artifacts in simulated images with a four element array. In addition, in vivo PILS imaging was demonstrated with a four element array at an acceleration factor of two with good image quality.

Table 1
SNR and Artifact Power in PILS

Acceleration:	1X	2X	3X
Relative SNR	0.9995 ± 0.0012	0.7197 ± 0.0132	0.5636 ± 0.0130
Relative SNR/time	0.9995 ± 0.002	1.0178 ± 0.026	0.9761 ± 0.026
Artifact power	8×10^{-9}	0.00066	0.022

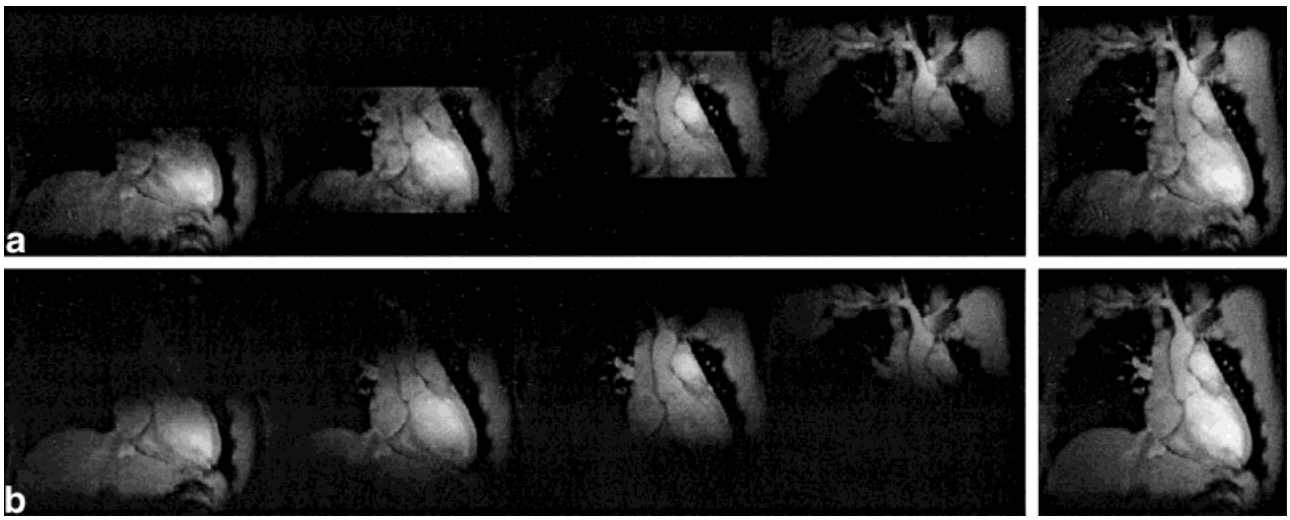

FIG. 9. In vivo PILS images acquired at an acceleration factor of two. **a:** PILS reconstruction. Note the nearly complete removal of aliasing artifacts from the composite image. **b:** The corresponding full time, fully gradient encoded reference images. Note that the PILS images in **a** have comparable image quality to those shown in **b**, which were acquired in twice the time.

All PPA techniques rely on two primary factors for successful reconstructions: (i) the spatial encoding performance of the imaging array; and (ii) the ability to measure the coil related parameters needed for the reconstruction, such as coil sensitivity maps. The primary difference between PILS and other PPA techniques is that the coil mapping procedure is simple and robust. Other methods require knowledge of the *coil sensitivity* at each location in the image (7) or along a single phase encoding line (2,14). The coil parameters required by PILS are relatively insensitive to noise and spin-density variations, since only the *position* of the center of each coil needs to be known exactly. While we have yet to observe any significant problems measuring the coil positions using this method, if a particular measured center position were severely contaminated with noise, the resulting subimage would be improperly shifted, resulting in local aliasing artifacts in the composite image. These artifacts can be corrected through post-processing by inspecting the component coil images, and shifting the affected coil center locations until the coil center is properly aligned with the component coil image.

One particular advantage of PILS compared to other PPA techniques is that the link between image artifacts and the reconstruction algorithm is clear. To date we have observed only two types of image artifacts resulting from the PILS reconstruction. The first artifact is an error in the measured coil center described above. If this error were to occur, it could be recognized by asymmetrical aliasing in a component coil image. The second, more common artifact is residual aliasing artifacts in the component coil images due to the extended field of the coils, which also appear in the composite image. This has the typical appearance of symmetrical aliasing in the component coil images (for example, Fig. 6a). While there is no easy way to correct this artifact after data acquisition, in PILS there is a simple cause and effect relationship. In PILS, this artifact can only be caused from an aliased signal from outside the small FOV. Therefore the solution to this artifact is simply to enlarge the FOV used in the small FOV images, either by increasing the target to full FOV size, or by decreasing the acceleration factor. In other PPA techniques, this relationship is not as clear, especially since the composite image is the only image available after reconstruction. Aliasing artifacts in these techniques may be caused either by the poor performance of the array or by inaccurate or incomplete coil mapping procedures (2,7). The inability to determine the exact cause of the aliasing artifact in these techniques can make the correction of the artifact more difficult.

Although determination of the relevant coil parameters is simplified in PILS, the reconstruction is more sensitive to the underlying coil performance than other techniques. The primary issue in this respect is the isolation of the elements in the array. Arrays with isolation on the order of 25–30 dBs between elements have been reported for numerous non-PILS applications (e.g., Ref. 17), so that dedicated PILS arrays with isolation on this order should be possible. Given the in vivo results presented in this study using an array with isolation on the order of 20 dBs (16), the technique is feasible at this level of isolation.

Another potential limitation of PILS is the requirement that the coils essentially act as filters along the phase encoding direction. In cases where the desired imaging plane does not correspond to the array direction, the performance of PILS will be greatly reduced. While this is a significant limitation, it is anticipated that the design of multidimensional arrays of coils could help alleviate this problem (2).

While the PILS technique can potentially be used to acquire images at acceleration factors approaching the number of array elements, it is clear that the performance of PILS is probably optimal at acceleration factors approximately equal to half the number of array elements. Above this level of acceleration, the technique is very dependent on the performance of the array for accurate image reconstructions. Therefore, we recommend using PILS in the lower range of acceleration factors. It should be stressed that this is the range of accelerations where all other PPA

techniques have been used to date, due as well to practical limitations which are only significant at the higher acceleration factors. In our experience, this is primarily due to the sensitivity of PPA techniques to errors in coil sensitivity mapping. While other PPA techniques have been shown to work at the maximum possible acceleration factor (i.e., the number of array elements) in phantom experiments, practical issues have prevented the application of these techniques at the maximum possible acceleration in vivo.

The primary advantages of PILS in this lower range of acceleration factors is the ease of coil parameter determination and image SNR. For example, the raw profiles used in this gaussian fit are heavily contaminated by both noise and spin density variations, such that the extraction of the pure coil sensitivity information is difficult in this case. However, as can be seen from this figure, the gaussian fitting technique used in this study gives reasonable values for the position of the center, even though the fit to the actual image intensities is relatively poor. An additional advantage is the ability to determine the coil related parameters from magnitude profiles, instead of the complex profiles needed in other PPA techniques, since PILS does not require information about the phase of the coils at any point in the reconstruction. This leads to more robust reconstructions, since the coil mapping routine used in PILS should not be susceptible to phase variations across the imaging slice.

All images reconstructed by PPA techniques necessarily have lower SNR than a fully encoded, slower acquisition. SNR is an area of critical importance for PPA techniques, since most fast imaging applications where PPAs will have the most impact (e.g., cardiac imaging) are already limited by SNR. In these cases, any additional losses introduced by the PPA reconstruction, besides the decrease in SNR due to the decreased acquisition time, cannot be easily tolerated. One advantage of PILS in this respect is that SNR in the PILS technique simply follows the decrease in SNR found in conventional MR imaging. This slight increase in SNR performance compared to other techniques can potentially be used to increase image quality or to investigate imaging problems which are more limited by SNR, such as cardiac perfusion measurements.

CONCLUSIONS

In this study we have presented a novel PPA method which requires minimal a priori knowledge of the RF coil array to reconstruct an image. We have demonstrated that the incorporation of simple coil parameters into a localized Fourier transform allows reconstruction of full FOV images in each of the component coils from data sets acquired with a reduced number of phase encoding steps, compared to conventional imaging techniques. This results in an increase in imaging speed. Simulated and in vivo images were shown which demonstrate the feasibility of PILS imaging. In addition to the low artifact powers in these reconstructions, the PILS technique was shown to have optimal SNR efficiency at all acceleration factors tested. Future work on PILS will concentrate on improving the performance of the technique at higher acceleration factors and on the development of array coils designed specifically for PILS imaging.

REFERENCES

1. Roemer PB, Edelstein WA, Hayes CE, Souza SP, Mueller, OM. The NMR phased array. Magn Reson Med 1990;16:192–225.
2. Sodickson DK, Manning WJ. Simultaneous acquisition of spatial harmonics (SMASH): fast imaging with radiofrequency coil arrays. Magn Reson Med 1997;38:591–603.
3. Jakob PM, Griswold MA, Edelman RR, Manning WJ, Sodickson DK. Accelerated cardiac imaging using the SMASH technique. J Cardiovasc Magn Reson 1999;1(2):153–157.
4. Sodickson DK, Bankson JA, Griswold MA, Wright SM. Eightfold improvements in MR imaging speed using SMASH with a multiplexed eight-element array. In: Proceedings of the 6th Annual Meeting of ISMRM, Sydney, Australia, 1998. p 577.
5. Bankson JA, Griswold MA, Wright SM, Sodickson DK. An eight-element linear array for SMASH imaging. In: Proceedings of the 6th Annual Meeting of ISMRM, Sydney, Australia, 1998. p 577.
6. Sodickson DK, Griswold MA, Jakob PM, Edelman RR, Manning WJ. Signal-to-noise ratio and signal-to-noise efficiency in SMASH imaging. Magn Reson Med 1999;41:1009–1022.
7. Prüssmann KP, Weiger M, Scheidegger MB, Boesiger P. SENSE: Sensitivity encoding for fast MRI. Magn Reson Med 1999;42(5):952–962.
8. Kelton J, Magin RM, Wright SM. An algorithm for rapid image acquisition using multiple receiver coils. In: Works in Progress, Proceedings of the 8th Scientific Meeting of SMRM, Amsterdam, 1989. p 1172.
9. Carlson JW, Minemura T. Imaging time reduction through multiple receiver data acquisition and image reconstruction. Magn Reson Med 1993;29:681–688.
10. Ra JB, Rim CY. Fast imaging using subencoding data sets from multiple detectors. Magn Reson Med 1993;30:142–145.
11. Wang J, Reykowski A. A SMASH/SENSE related method using ratios of array coil profiles. In: Proceedings of the 7th Annual Meeting of ISMRM, Philadelphia, 1999. p 1648.
12. Weiger M, Prüssmann KP, Boesiger P. High performance cardiac realtime imaging using SENSE. In: Proceedings of the 7th Annual Meeting of ISMRM, Philadelphia, 1999. p 385.
13. Dydak U, Weiger W, Prüssmann KP, Van Den Brink J, Lamerichs R, Meier D, Boesiger P. Scan time reduction in spectroscopic imaging using SENSE. In: Proceedings of the 7th Annual Meeting of ISMRM, Philadelphia, 1999. p 679.
14. Jakob PM, Griswold MA, Edelman RR, Sodickson DK. AUTO-SMASH: a self-calibrating technique for SMASH imaging. MAGMA 1998;7:42–54.
15. Edelstein WA, Foster TH, Schenck JH. The relative sensitivity of surface coils to deep lying tissues. In: Proceedings of the 4th Annual Meeting of the SMRM, London, 1985. p 410.
16. Griswold MA, Jakob PM, Edelman RR, Sodickson DK. An RF coil array designed specifically for cardiac SMASH imaging. In: Proceedings of the 6th Annual Meeting of ISMRM, Sydney, Australia, 1998. p 437.
17. Duensing GR, Peterson DM, Wolverton BL, Fitzsimmons JR. Transceive phased array designed for imaging at 3.0T. In: Proceedings of the 6th Annual Meeting of ISMRM, Sydney, Australia, 1998. p 441.